Electronic supplementary information

Regulation of clusterization-triggered phosphorescence from non-conjugated amorphous polymer: a platform for colorful afterglow

Shuaiqi Wang, Duobin Wu, Shuming Yang, Zhenghuan Lin*, and Qidan Ling

Fujian Key Laboratory of Polymer Materials, College of Chemistry and Materials Science, Fujian Normal University, Fuzhou 350007, China.
Email: zhlin@fjnu.edu.cn

Table S1 Synthetic conditions and photophysical data of various PAMs.

	Initiator	T (°C)	Time (h)	M_w (KDa)	PDI	λ_{em}[c] (nm)	λ_{em}[d] (nm)	τ[d] (ms)	Φ %
PAM1	AIBN	65	24	5	2.61	390	/	/	1.81
PAM2	$(NH_4)_2S_2O_8$	100	24	280	5.13	390	485	155	14.1
PAM3	$(NH_4)_2S_2O_8$	100	48	324	6.56	399	482	219	24.3
PAM4[a]	Na_2SO_3/ $(NH_4)_2S_2O_8$	25	12	326	3.04	389	475 / 540	224 / 188	10.3
PAM5[b]	Na_2SO_3/ $(NH_4)_2S_2O_8$	25	12	386	3.94	398	481	361	20.0

[a] Without aging treatment; [b] With aging treatment; [c] Emission wavelength of fluorescence; [d] Emission wavelength of phosphorescence.
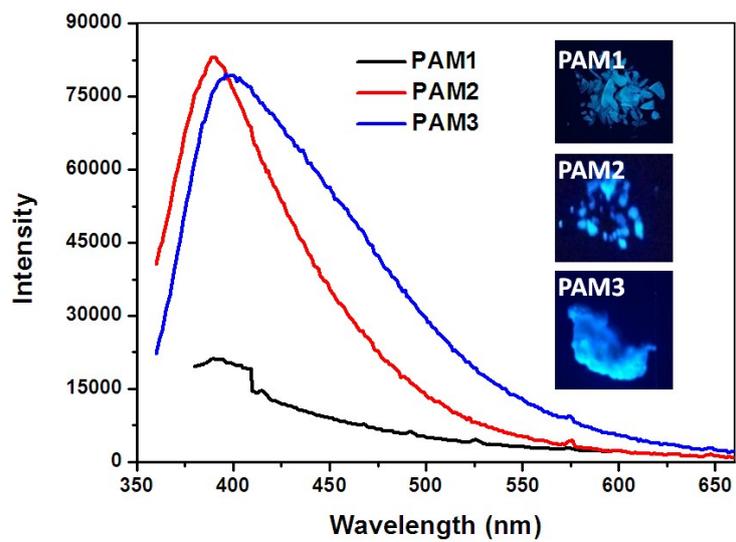
Fig. S1 Emission spectra of PAM1-PAM3 excited at 365 nm. Inset: their photographs taken under 365 nm of UV light.
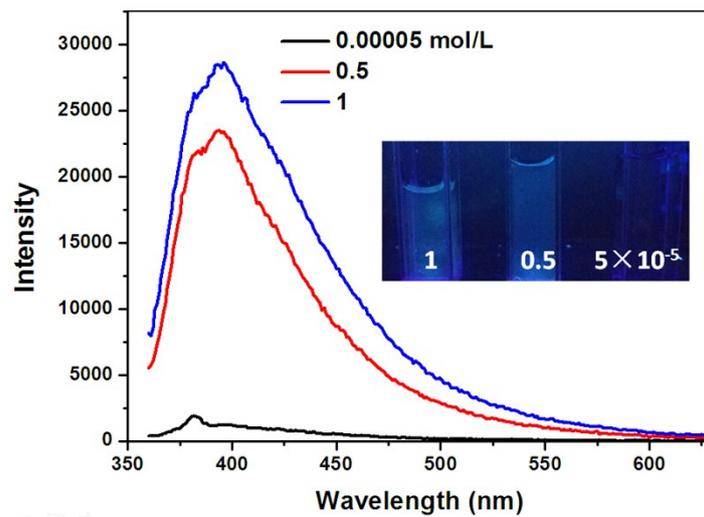
Fig. S2 Emission spectra of PAM3 in different concentration of aqueous solution. Inset: their photographs taken under 365 nm of UV light.
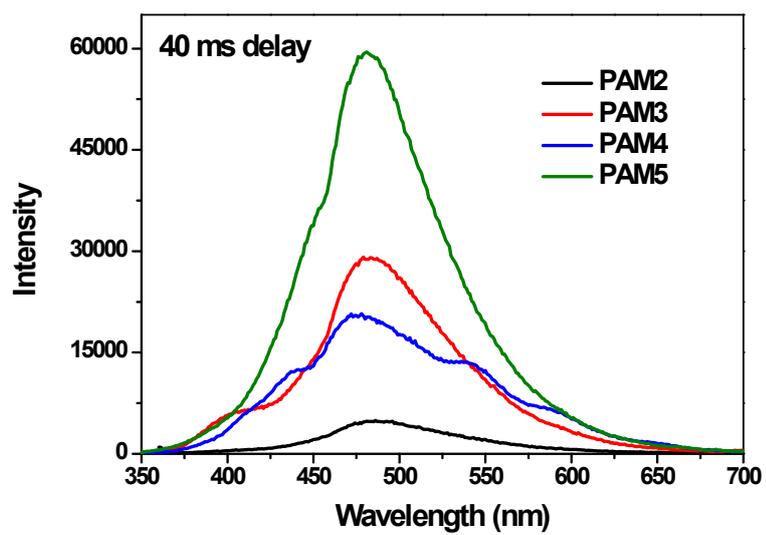
Fig. S3 Delay emission spectra of PAM2-PAM5.
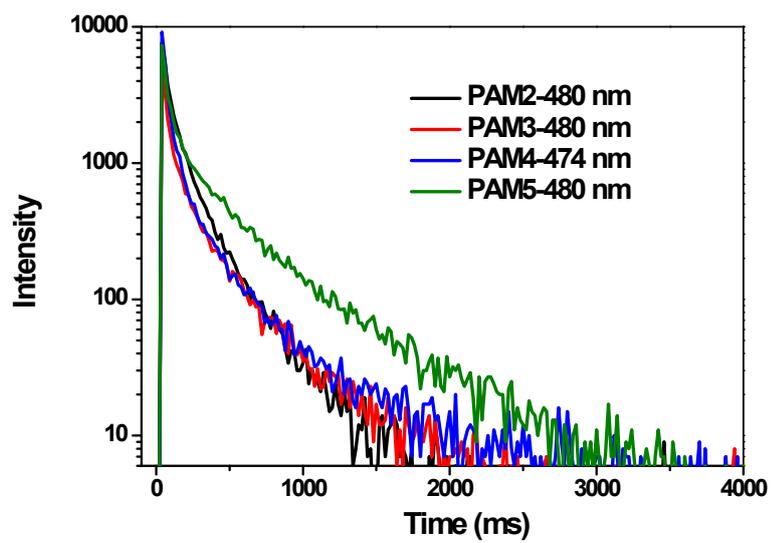
Fig. S4 Transient luminescence decays of PAM2-PAM5 monitored at about 480 nm.

Table S2 Lifetime data of PAM2-PAM5.

Polymer	λ_{em} (nm)	τ_1 (ms)	τ_2 (ms)	τ_3 (ms)	τ_{av} (ms)	χ^2
PAM2	480	19.87 (15.88%)	99.10 (50.30%)	302.67 (33.82%)	155.37	1.042
PAM3	480	26.36 (25.31%)	146.14 (45.34%)	497.34 (29.35%)	218.90	1.055
PAM4	474	30.39 (41.64%)	181.58 (43.67%)	898.99 (14.69%)	224.01	1.061
	540	19.46 (27.78%)	105.37 (37.47%)	410.78 (34.75%)	187.63	1.025
	590	18.10 (24.35%)	95.60 (31.11%)	369.03 (44.54%)	198.07	1.016
PAM5	480	33.99 (21.39%)	236.43 (40.91%)	682.93 (37.7%)	361.46	1.003
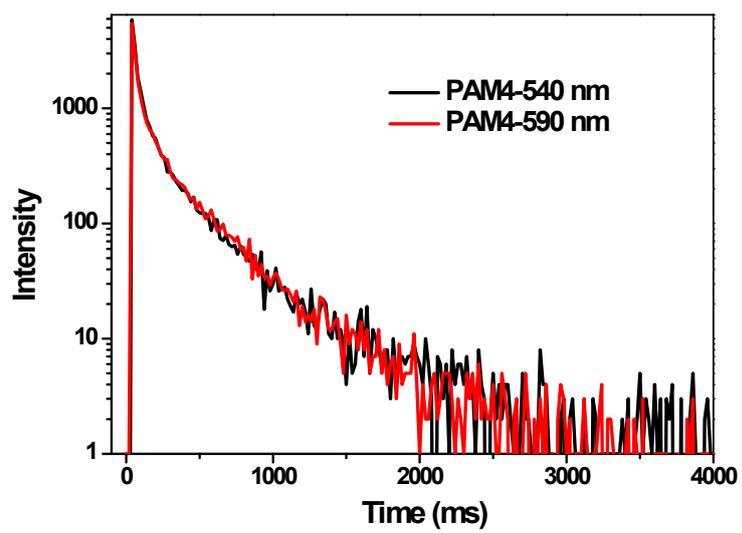
Fig. S5 Transient luminescence decays of PAM4 monitored at 540 nm and 590 nm.

Table S3 Amount of elements C, H and N in PAMs.

	C	H	N
PAM (calc.)	50.69	7.09	19.71
PAM2	50.17	7.20	18.00
PAM3	50.25	7.13	19.31
PAM4	50.10	8.12	19.49
PAM5	50.22	8.30	19.29
PAM-N1	51.35	7.86	19.6
PAM-N2	51.33	7.79	19.43
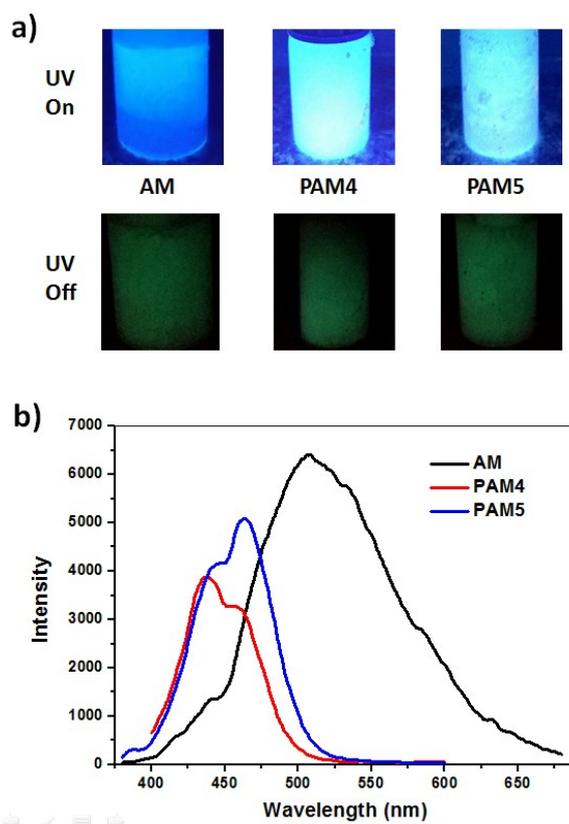
Fig. S6 a) Photos of AM, PAM4 and PAM5 in dilute aqueous solution (1 μM) at 77 K, taken under 365 nm of UV light, and after turn-off UV light. b) Their phosphorescence spectra excited at 347 nm.
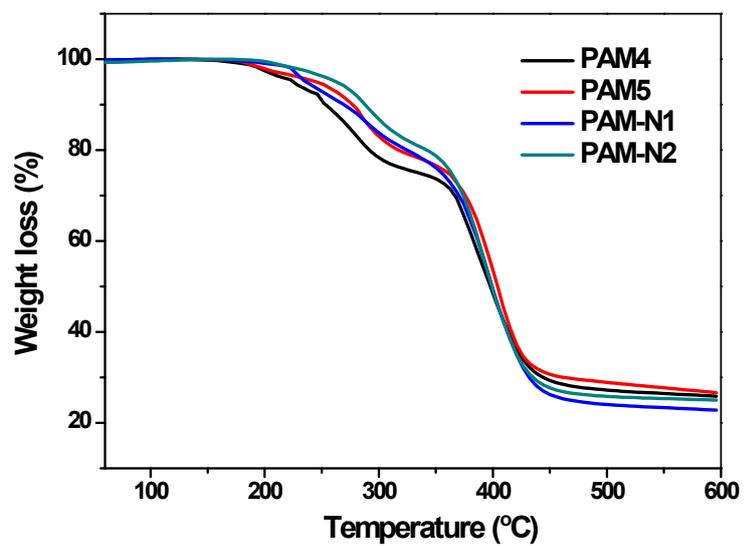
Fig. S7 Thermogravimetric (TG) analysis of PAM4, PAM5, PAM-N1 and PAM-N2.
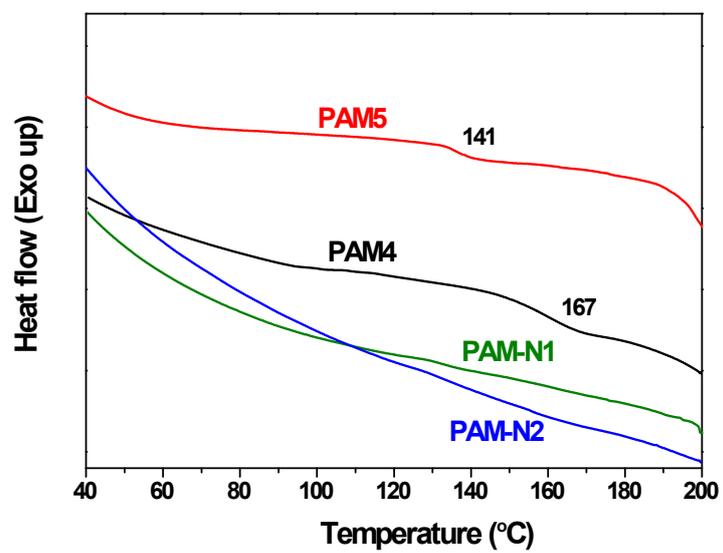
Fig. S8 Differential scanning calorimetry (DSC) analysis of PAM4, PAM5, PAM-N1 and PAM-N2.

Table S4 Triplet excited state transition configurations of structural units obtained by TD-DFT calculations.

	Energy, (eV)	λ, nm	f	Main orbital transition[a] (CIC)
AM1	1.84	672	0.0007	LUMO→HOMO (0.71)
AM2	2.69	461	0.0050	LUMO→HOMO (0.69) LUMO→HOMO-2 (0.14)
AM3	2.81	442	0.0053	LUMO→HOMO (0.68) LUMO→HOMO-2 (0.15)
AM1-1	1.49	831	0.0015	LUMO→HOMO (0.70)
AM2-2	2.11	587	0.0039	LUMO→HOMO (0.69) LUMO→HOMO-5 (0.10)
AM3-3	1.98	627	0.0035	LUMO→HOMO (0.69)

[a] CI expansion coefficients for the main orbital transitions.
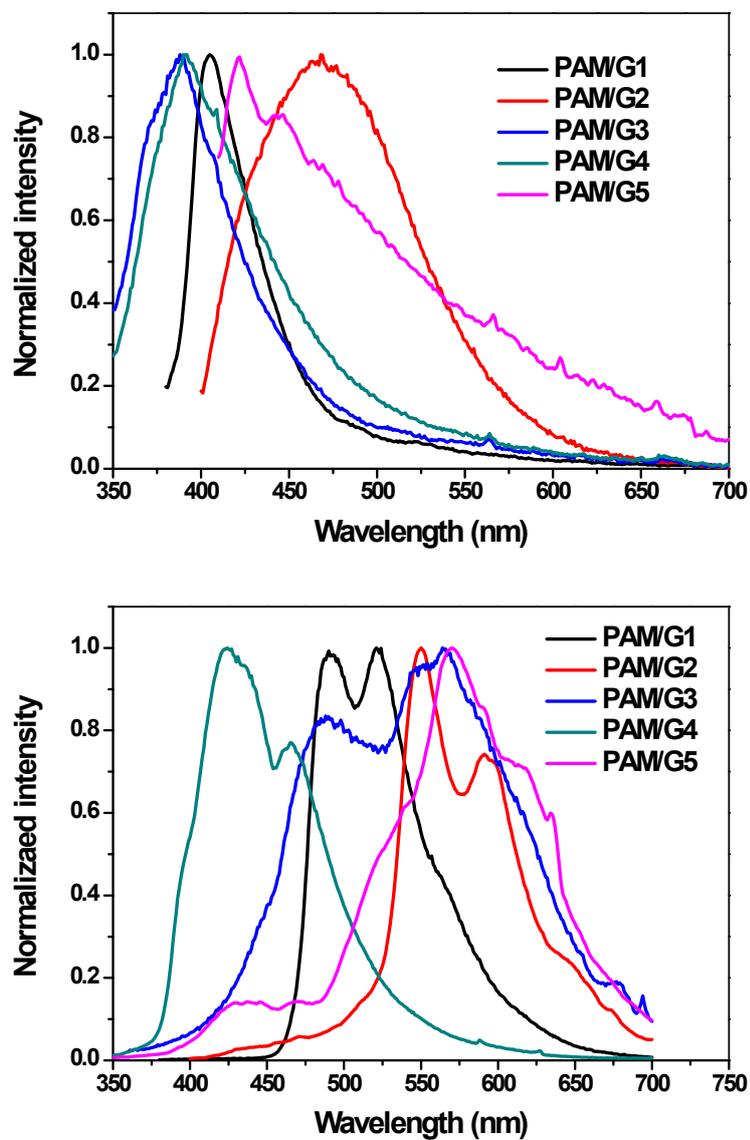
Fig. S9 Prompt (upper) and delay (bottom) emission spectra of PAM/G1-PAM/G5.

Table S5 Reported triplet energy of G1-G5 luminophores.

	Luminophore	Energy, (eV)	λ, nm	Reference
G1	2,3-Naphthalimide	2.36	526	1
G2	1,8-Naphthalimide	2.24	554	2, 3
G3	Maleimide	2.31	537	4, 5
G4	Terephthalic acid	2.58	480	6
G5	Naphthalene diimide	2.03	610	7
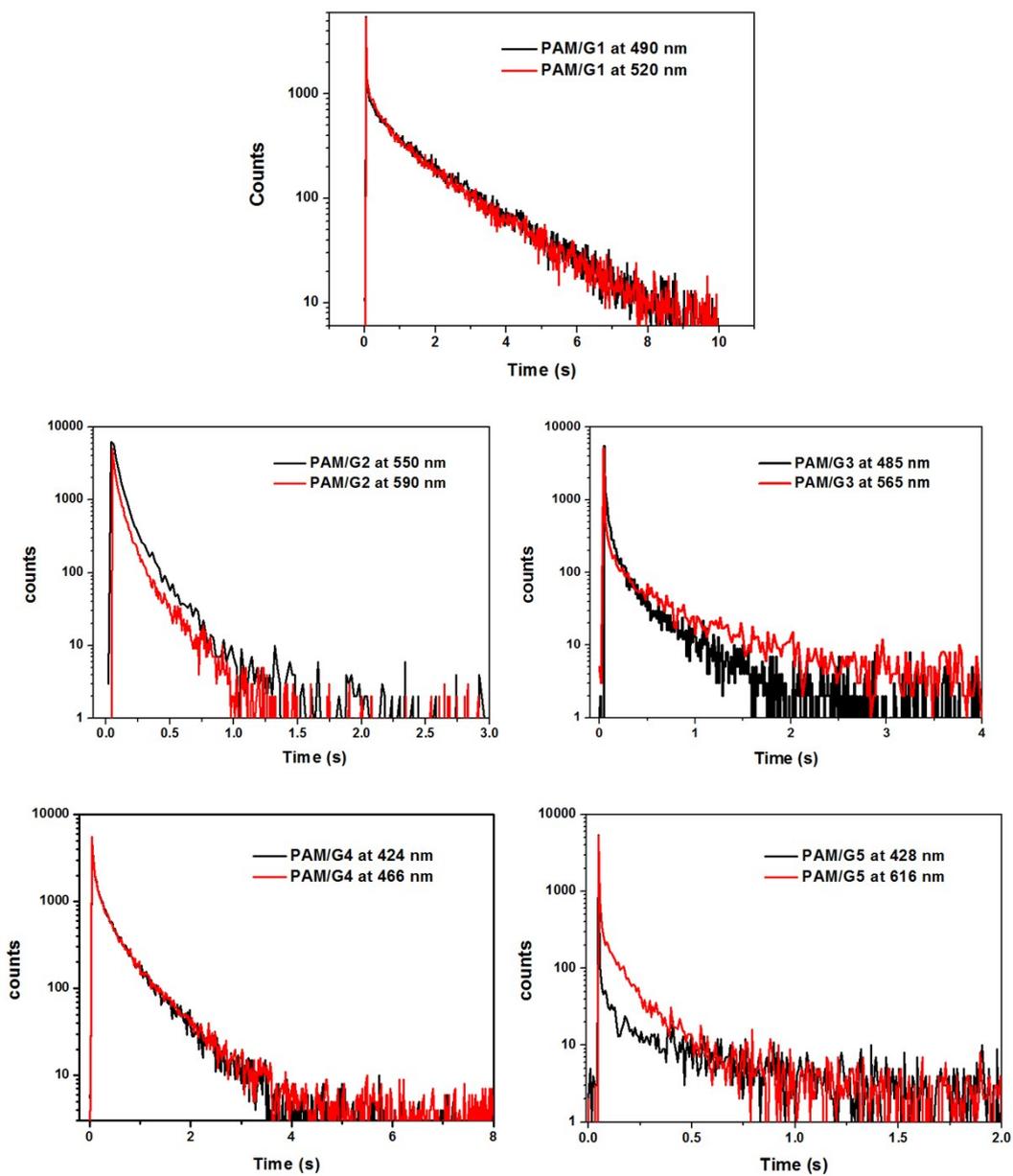
Fig. S10 Transient luminescence decays of PAM/G1-PAM/G5 monitored at different emissive peaks.

Table S6 Photophysical properties of PAM/G1-PAM/G5 in solids.

Polymer	λ_{ex} (nm)	λ_{em} (nm)	τ (ms)	Φ %
PAM/G1	365	490	1701.6	13.4
		520	1319.9	
PAM/G2	365	550	120.87	16.5
		590	86.14	
PAM/G3	334	485	169.14	3.93
		565	469.76	
PAM/G4	333	424	427.1	13.4
		466	450.4	
PAM/G5	308	428	291.74	0.22
		616	251.69	

Scheme S1 Synthetic routes of PAM-N1 and PAM-N2.
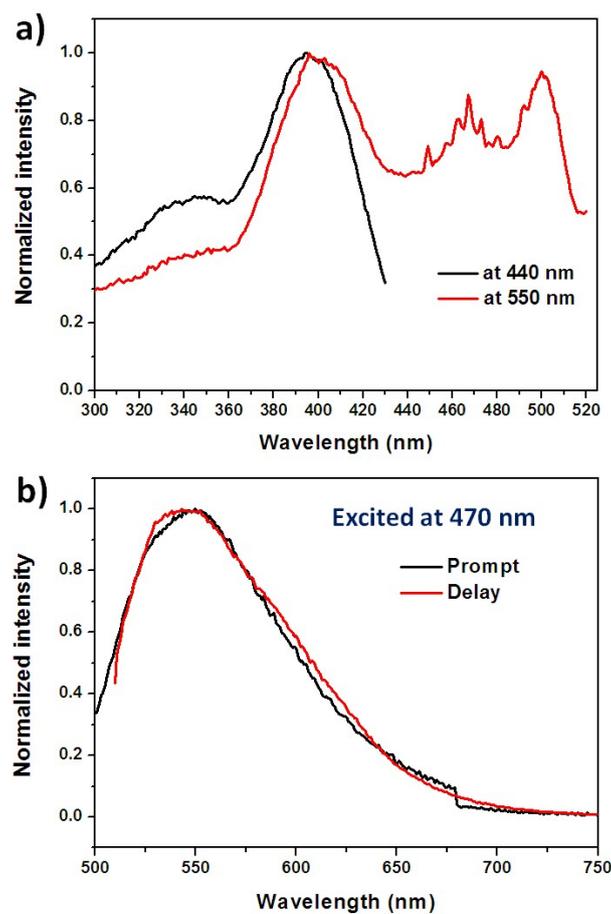
Fig. S11 (a) Excitation spectra of PAM-N2 monitored at 440 nm and 550 nm. (b) Prompt and delay emission spectra of PAM-N2 excited at 470 nm.
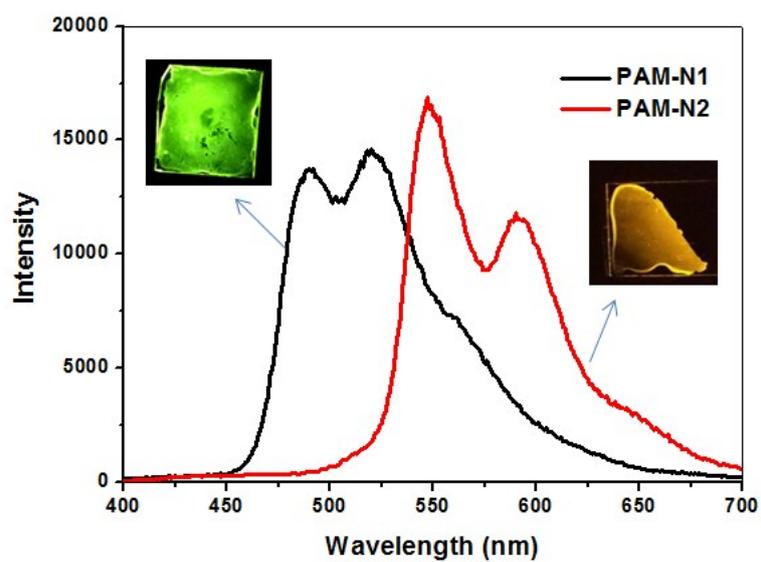
Fig. S12 Delay emission spectra of PAM-N1 and PAM-N2 in films excited at 365 nm and 347 nm respectively. Inset: their photos taken after turn-off of a 365 nm of UV lamp.
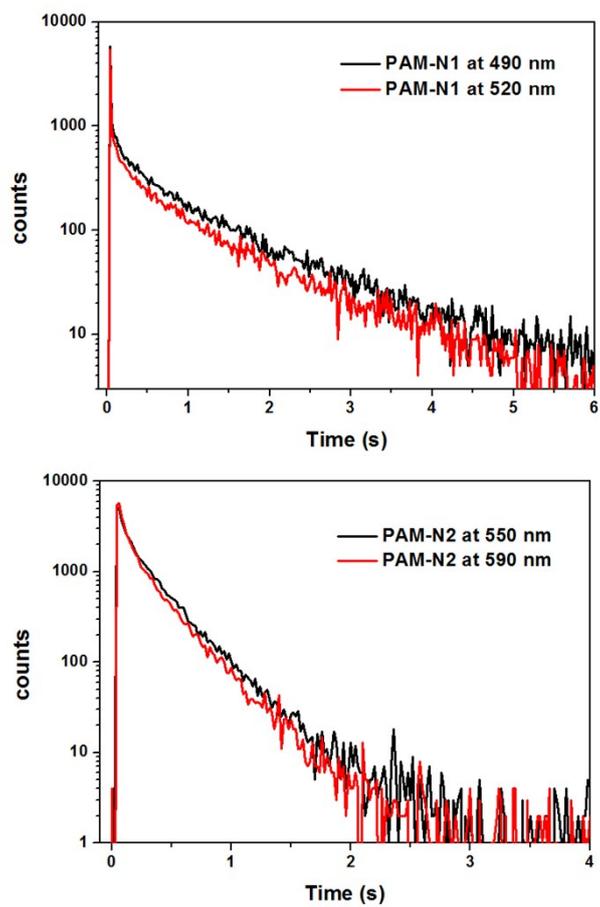
Fig. S13 Transient luminescence decays of PAM-N1 and PAM-N2 in films monitored at different emissive peaks.
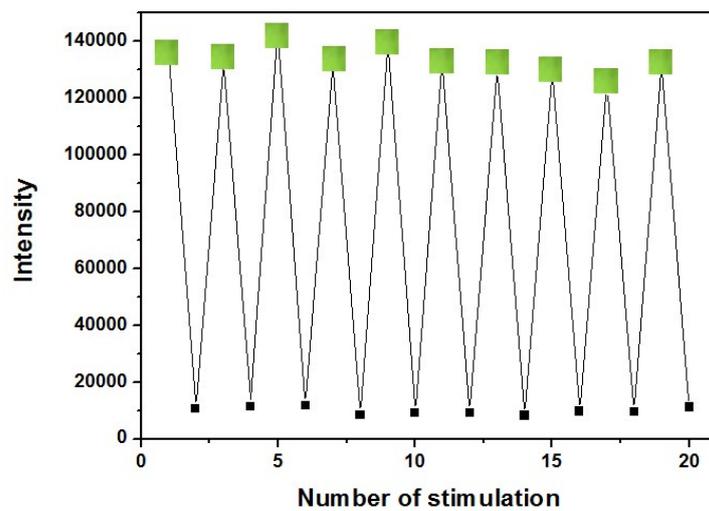
Fig. S14 Repeatability of afterglow switching under alternating stimulation of NH$_3$ vapor and heating.
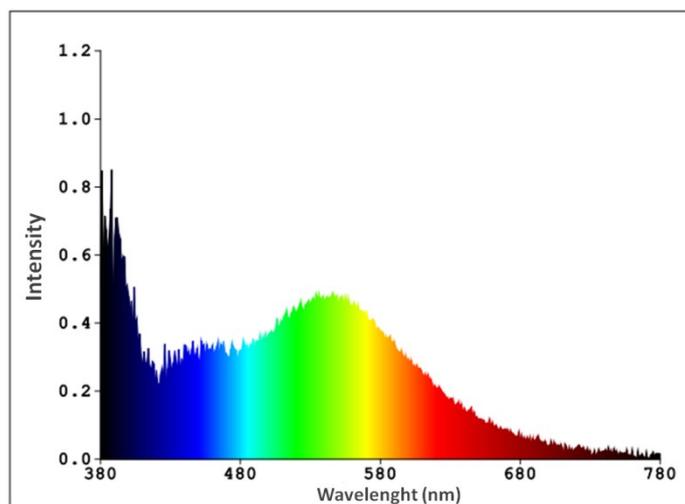
Fig. S15 Electroluminescence spectra of LED based on PAM-N2.

Experimental section

Materials

All chemicals were obtained from commercial suppliers and used directly in the experiments without further purification unless otherwise stated. G1 and G2 were synthesized according to the reported procedures.[2] Compounds G1-G4 were purified by recrystallization with ethyl acetate. G5 was purified by recrystallization with DMF.

Measurements

NMR spectra were measured on a Bruker Ascend 400 FT-NMR spectrometer. ^{1}H NMR spectra were quoted relative to the internal standard tetramethylsilane. The molecular weight of all polymers was measured by Shimadzu rid-20a (GPC) with LC20 high performance liquid chromatography pump and rid-20 differential refraction detector. 0.1M $NaNO_3$ and 0.06% NaN_3 aqueous solution was used as the mobile phase at 0.6 mL min^{-1} flow rate. Steady-state photoluminescence spectra and quantum yield of the samples were obtained at the room temperature using an Edinburgh FS5 spectrofluorometer with a xenon arc lamp (Xe900) and an integrating sphere for absolute photoluminescence quantum yield determination. Time-resolved photoluminescence decay curves and delay spectra were obtained using a FLS920 Fluorescence Spectrometer equipped with a microsecond flash-lamp (μF900), and a nanosecond hydrogen flash-lamp (nF920). TGA and DSC data were obtained from Mettler's thermogravimeter and differential scanning calorimeter, respectively. The heating rate is 10 ^{o}C/min, nitrogen is used to protect the test process. Element analysis data were obtained from Vario EL Cube (Elementar, Germany).

Computational Methods

Molecular Simulations were performed on Gaussian 09 program. Geometry at ground state was fully optimized by the density functional theory (DFT) method with the Becke three-parameter hybrid exchange and the Lee-Yang-Parr correlation functional (B3LYP) and 6-31G* basis set. The triplet excited state transition configurations were revealed by time-dependent DFT (TD-DFT) using same functional and basis sets.

Synthesis of PAM1

The polymer was prepared by free-radical solution polymerization from acrylamide (1.0 g, 14.06 mmol) and 2,2'-azobis(2-methylpropionitrile) (AIBN) (4.6 mg, 0.028 mmol). The reaction was performed in 10 mL of DMF/H_2O (100/1, v/v) at 65 °C under an nitrogen atmosphere for 24 h. The resulting mixture was added into methanol to precipitate. Precipitate was repeatedly washed with methanol, and dried at 80 °C in a vacuum oven to give the pure polymer. GPC (H_2O): M_n (PDI) = 2.0 kDa (2.61).

Synthesis of PAM2 and PAM3

The polymer was prepared by free-radical solution polymerization from acrylamide (0.5 g, 7.03 mmol) and $(NH_4)_2S_2O_8$ (3.2 mg, 0.014 mmol). The reaction was performed in 5 mL of H_2O at 100 °C under an nitrogen atmosphere for 24 h (for PAM2) or 48 h (for PAM3). The resulting mixture was added into methanol to precipitate. Precipitate was repeatedly washed with methanol, and dried at 80 °C in a vacuum oven to give the pure polymer. GPC (H_2O) of PAM2: M_n (PDI) = 55 KDa (5.13). GPC (H_2O) of PAM3: Mn (PDI) = 50 KDa (6.56).

Synthesis of PAM4 and PAM5

The polymer was prepared by free-radical solution polymerization from acrylamide (0.5 g, 7.03 mmol) and $(NH_4)_2S_2O_8$/Na_2SO_3 (1.6 mg/0.9 mg). The reaction was performed in 5 mL of H_2O at room temperature under an nitrogen atmosphere for 12 h. The resulting mixture without (for PAM4) and with (for PAM5) an additional aging at 100 °C for 2h was added into methanol to precipitate. Precipitate was repeatedly washed with methanol, and dried at 80 °C in a vacuum oven to give the pure polymer. GPC (H_2O) of PAM4: M_n (PDI) = 107 KDa (3.04). GPC (H_2O) of PAM5: Mn (PDI) = 98 KDa (3.94).

Preparation of PAM/G1- PAM/G5

Guest compound (0.028 mmol) was dissolved in 0.5 mL of water (for G1, G2 and G3) or DMF (for G4 and G5) and added to 2 mL of stirred PAM5 aqueous solution (0.57 N). Then the mixture solution was poured into methanol solution to give the blend polymer solid.

Synthesis of monomer N1 and N2

2,3-Naphthalimide (or 1,8-Naphthalimide) (2.54 mmol) and potassium carbonate (0.70 g, 5.08 mmol) were added to 25 mL of MeCN, and stirred at room temperature for 1h, followed by adding propylene bromide (0.37 g, 3.0 mmol). The mixture was stirred under reflux for 12 h, and extracted with ethyl acetate and washed with saturated salt water. The organic phase was

separated and dried over anhydrous magnesium sulfate. After the solvent was removed, the crude product was purified by recrystallization in ethyl acetate to give the pure compound, *N*-allyl-2,3-naphthalimide (N1) or *N*-allyl-1,8-naphthalimide (N2). N1: ^{1}H NMR (400 MHz, Chloroform-*d*) δ 8.38 (s, 2H), 8.09 (dd, *J* = 6.2, 3.3 Hz, 2H), 7.73 (dd, *J* = 6.2, 3.2 Hz, 2H), 6.05 – 5.91 (m, 1H), 5.38 – 5.17 (m, 2H), 4.39 (d, *J* = 5.7 Hz, 2H). N2: ^{1}H NMR (400 MHz, Chloroform-*d*) δ 8.66 (d, 2H), 8.26 (d, 2H), 7.79 (t, 2H), 6.06 – 6.02 (m, 1H), 5.33 (d, 1H), 5.22 (d, 1H), 4.85 (td, 2H).

Preparation of PAM-N1 and PAM-N2 copolymers

Two copolymers were prepared by radial copolymerization from acrylamide with N1 or N2, according to the same method and procedure as PAM5. GPC (H_2O) of PAM-N1: M_n (PDI) = 79 KDa (2.86). GPC (H_2O) of PAM-N2: M_n (PDI) = 47 KDa (5.19).
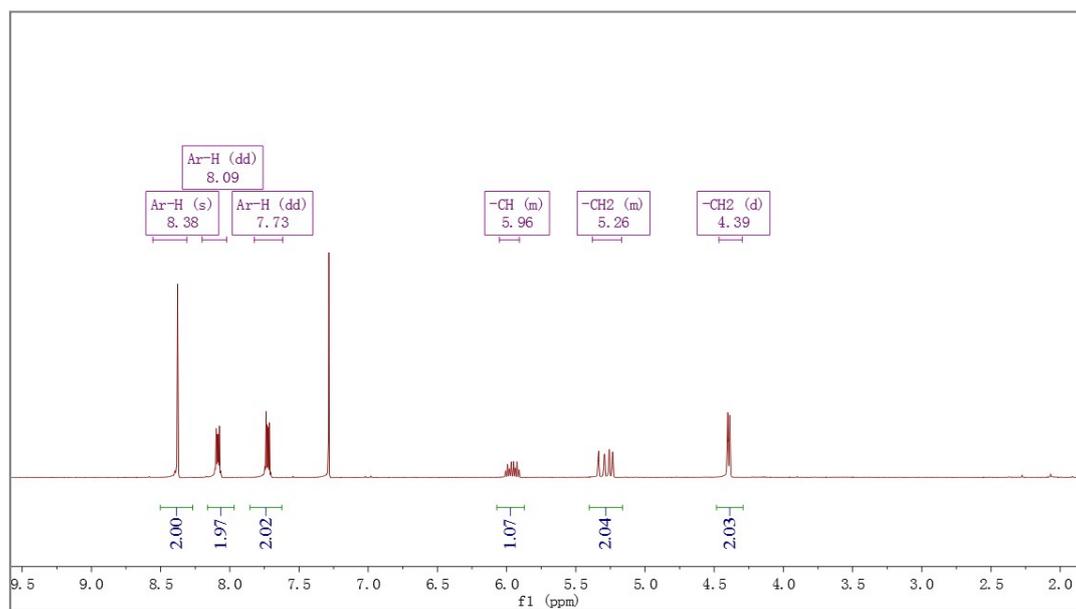
Fig. S16 ^{1}H NMR of N1 in *d*-Chloroform.
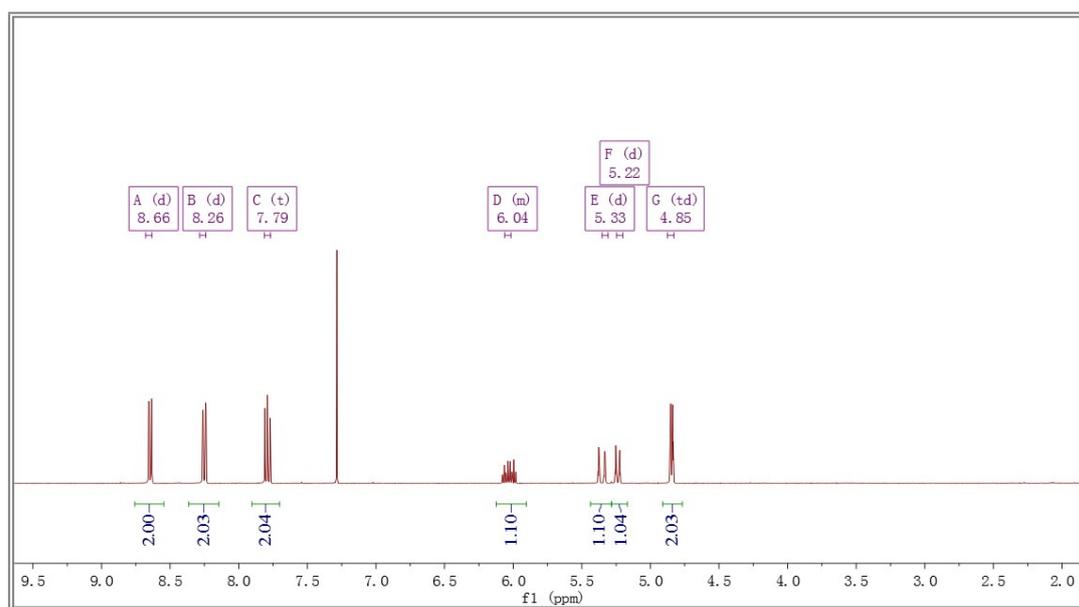
Fig. S17 ^{1}H NMR of N2 in *d*-Chloroform.
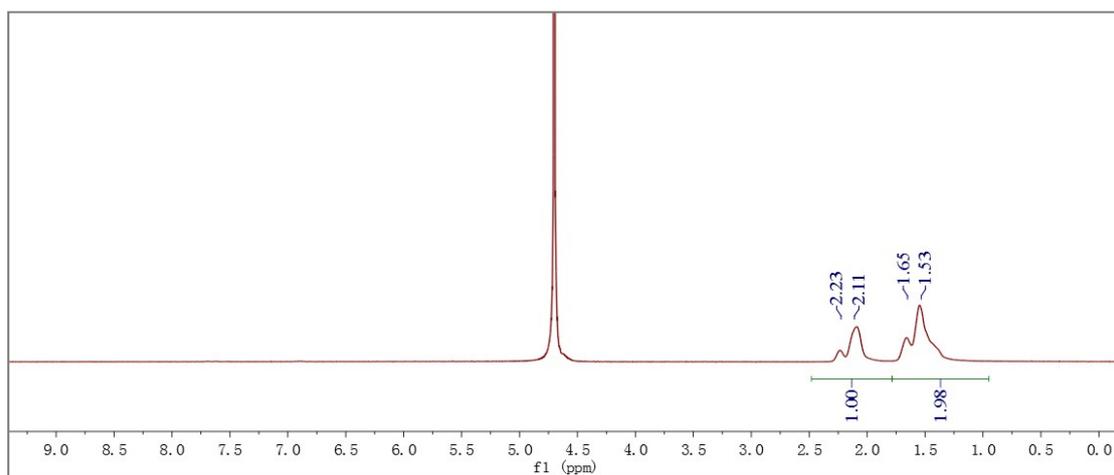
Fig. S18 ¹H NMR of PAM1 in D₂O.
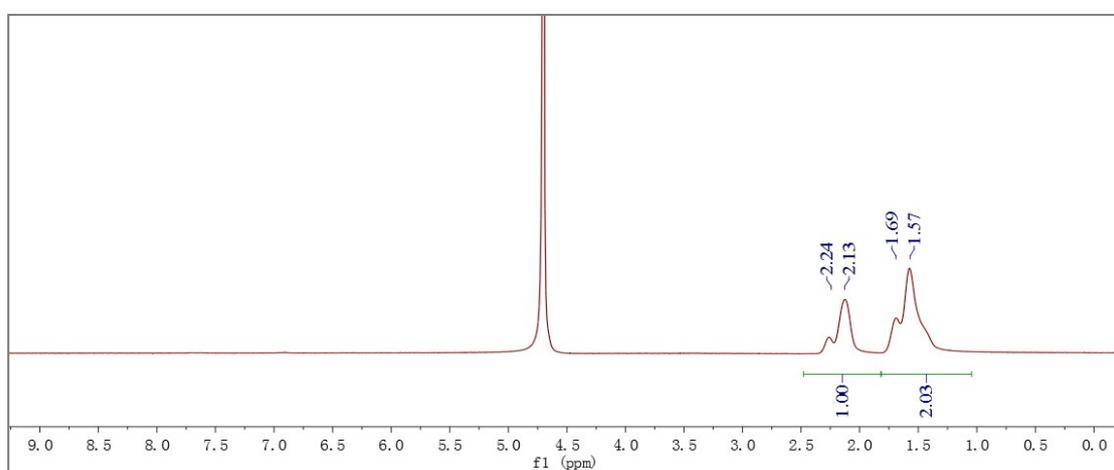
Fig. S19 ¹H NMR of PAM2 in D₂O.
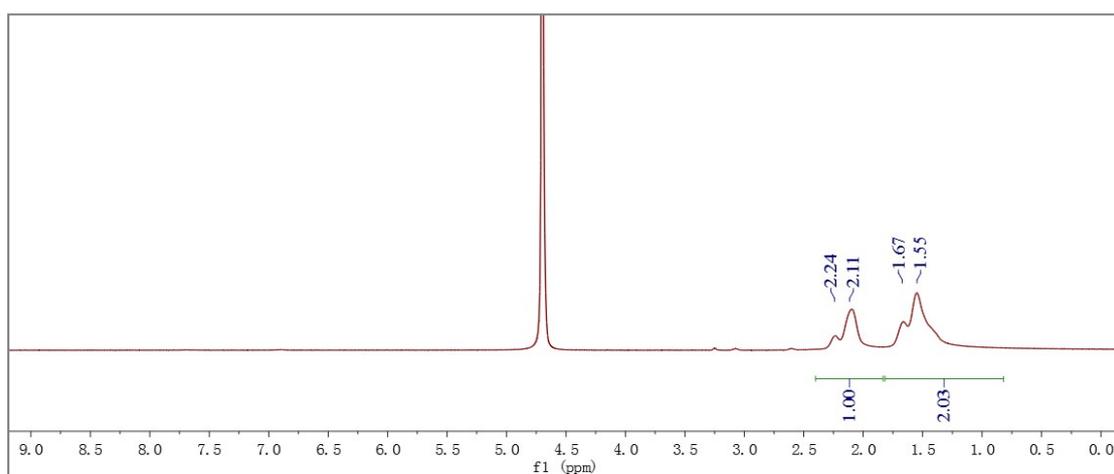
Fig. S20 ¹H NMR of PAM3 in D₂O.
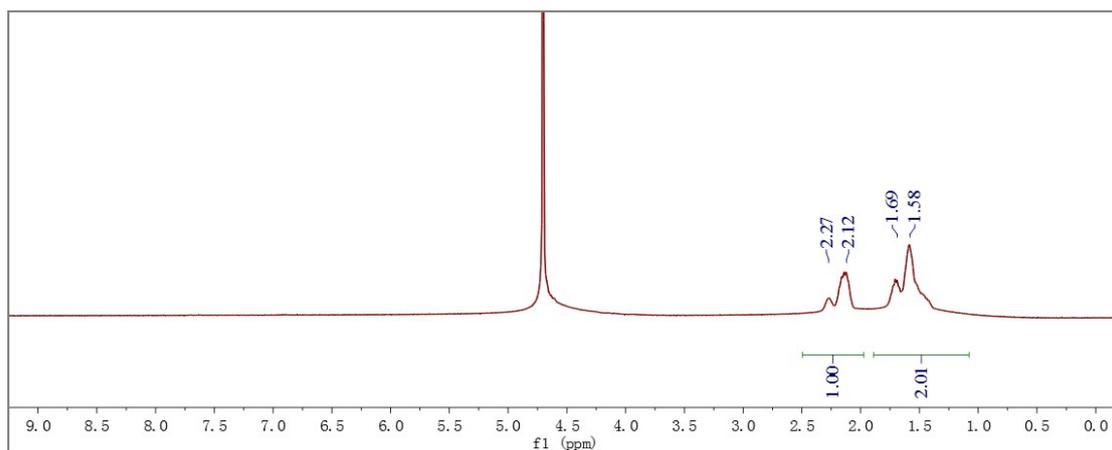
Fig. S21 ^{1}H NMR of PAM4 in D_2O.
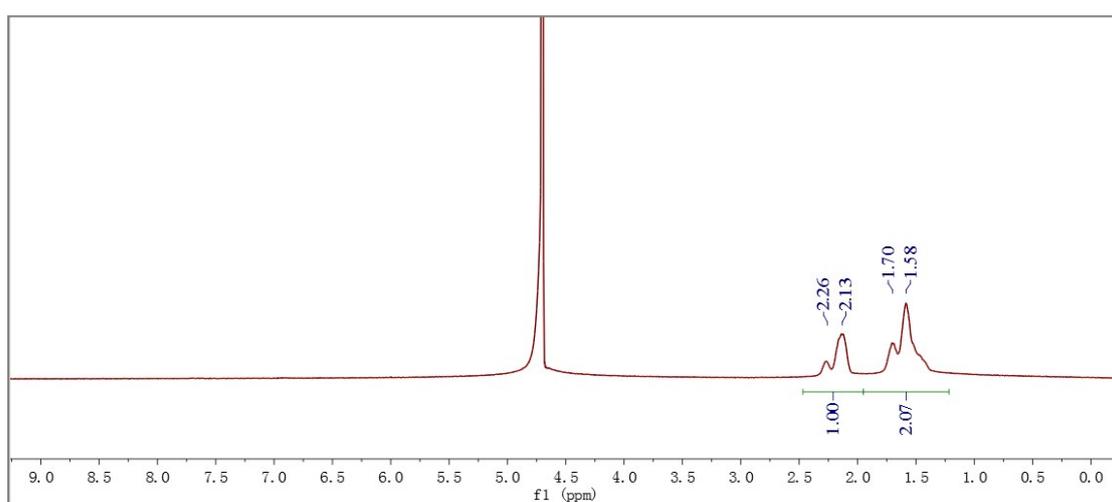
Fig. S22 ^{1}H NMR of PAM5 in D_2O.
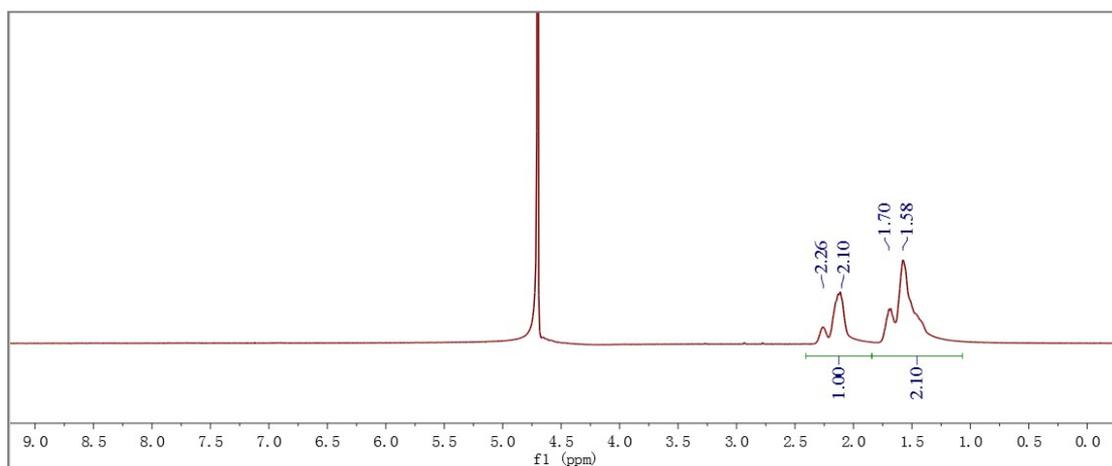
Fig. S23 ^{1}H NMR of PAM-N1 in D$_2$O.
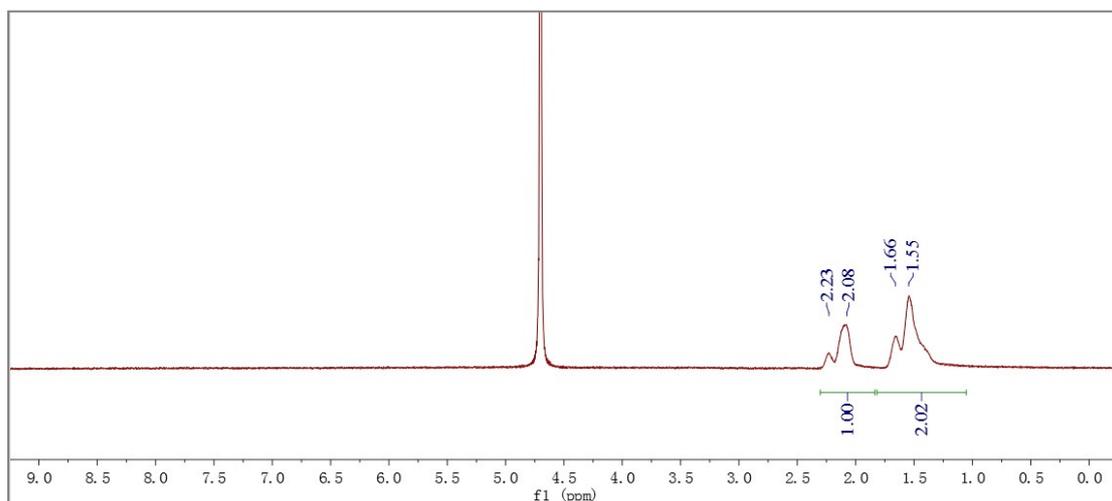
Fig. S24 ^{1}H NMR of PAM-N2 in D$_2$O.

References

1 P. Valat, V. Wintgens, J. Kossanyi, L. Biczok, A. Demeter and T. Berces, Influence of Geometry on the Emitting Properties of 2,3-Naphthalimides, *J. Am. Chem. Soc.* 1992, **114**, 946-953.

2 S. Yang, D. Wu, W. Gong, Q. Huang, H. Zhen, Q. Ling and Z. Lin, Highly efficient room-temperature phosphorescence and afterglow luminescence from common organic fluorophores in 2D hybrid perovskites, *Chem. Sci.* 2018, **9**, 8975-8981.

3 B. Ventura, A. Bertocco, D. Braga, L. Catalano, S. d'Agostino, F. Grepioni and P. Taddei, Luminescence Properties of 1,8-Naphthalimide Derivatives in Solution, in Their Crystals, and in Co-crystals: Toward Room-Temperature Phosphorescence from Organic Materials, *J. Phys. Chem. C* 2014, **118**, 18646-18658.

4 T. Climent, R. González-Luque and M. Merchán, Theoretical Analysis of the Excited States in Maleimide, *J. Phys. Chem. A* 2003, **107**, 6995-7003.

5 C. J. Seliskar and S. P. McGlynn, Electronic Spectroscopy of Maleimide and Its Isoelectronic Molecules. I. Maleimide and N-Alkylmaleimides, *J. Chem. Phys.* 1971, **55**, 4337-4342.

6 R. Gao and D. Yan, Layered host–guest long-afterglow ultrathin nanosheets: high-efficiency phosphorescence energy transfer at 2D confined interface, *Chem. Sci.* 2017, **8**, 590-599.

7 J. Z. Liao, L. Meng, J. H. Jia, D. Liang, X. L. Chen, R. M. Yu, X. F. Kuang and C. Z. Lu, Anion-π Interaction-Induced Room-Temperature Phosphorescence of a Polyoxometalate-Based Charge-Transfer Hybrid Material, *Chem. Eur. J.* 2018, **24**, 10498-10502.